

Variation of self-energy and exciton-phonon coupling in KI and RbI with pressure

M. J. Lipp, J. Blechschmidt,* and W. B. Daniels

Department of Physics and Astronomy, University of Delaware, Newark, Delaware 19716

(Received 24 February 1993)

We measured the $1s$ exciton energies in KI and RbI versus temperature at three different pressures via three-photon-excitation spectroscopy. The observed excitations display a Lorentzian line shape, which can be viewed as evidence that excitons and phonons in KI and RbI are only weakly coupling. Using the weak-coupling model we were able to find values for the real part of the temperature-dependent self-energy of the $1s$ exciton (peak-shift parameter Δ). We find that the absolute value of Δ and the strength of the exciton-phonon coupling increase with pressure. We also studied the behavior of the linewidth of the $1s$ exciton-polariton resonance with pressure and temperature and found that it decreases with pressure. However, we do not think that the linewidth parameter Γ of the polariton can be rigorously interpreted as the imaginary part of the exciton self-energy.

I. INTRODUCTION

Recently we reported the use of three-photon-absorption spectroscopy¹ to investigate the $n=1$ exciton-polariton resonance structure of KI under hydrostatic high pressure.² We observed the pressure-induced blueshift of the $n=1$ longitudinal energies and a decrease in the curvature at $k=0$ of the transverse polariton branch lying between E_{1L} and E_{2T} . It was also found that the linewidth of the excitation maxima decreased significantly with increasing pressure. Subsequently, similar observations have been made for RbI.³

Figure 1 schematically shows the polariton dispersion relation for KI near the center of the Brillouin zone for the energy region from below the lowest triplet exciton with energy E_p to the band-gap energy (the dispersion relation for RbI looks qualitatively the same). The s excitons [with intrinsic energies E_{nT} (dashed lines)] are singlet-triplet mixed states, which can easily couple to the electromagnetic field of photons, resulting in the formation of exciton-polariton resonances whose dispersion curve is shown by the solid line. This coupling also introduces the longitudinal-transverse splitting between the upper (energy greater than E_{nL}) and lower polariton branches (energy smaller than E_{nT}). The behavior of the triplet exciton with pressure has been discussed elsewhere⁴ and is not of importance for the following discussions.

The dotted points in Fig. 1 show excitations that were observed in the present investigation. Those with a wave vector $k \approx 5.1 \times 10^7 \text{ m}^{-1}$ correspond to three polaritons each with about $1.7 \times 10^7 \text{ m}^{-1}$ and energy $E/3$ fusing together in the forward direction, called transverse polaritons TP($3k$), whereas the TP(k) are generated when one of the three polaritons is reflected at the backside of the crystal or the cell window, thus creating a polariton still having total energy E , but now the total wave vector $k \approx 1.7 \times 10^7 \text{ m}^{-1}$ ($=2k - k$).

Figure 2 displays a typical RbI excitation spectrum of the $n=1$ polariton [TP₁(k) and TP₁($3k$)] covering the

energy range from about 5.8 to 6.05 eV at two pressures. Knowing the energies E_{1T} and E_{1L} at different temperatures and pressures, it was possible to establish values for the excitonic self-energy and the strength of the exciton-phonon coupling as well as their changes with pressure. Table I contains the most recently measured values of the $1s$ excitonic energies and their pressure dependence for RbI and KI.

II. EXPERIMENTAL ASPECTS

A major obstacle in interpreting *one-photon* absorption or reflection spectra is that the inherently large (large in comparison to multiphoton techniques) k vector

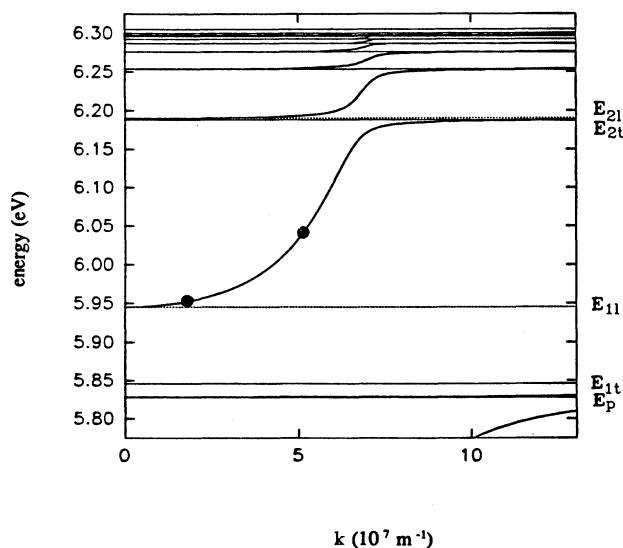


FIG. 1. Dispersion relation of the polaritons near the center of the Brillouin zone for KI. The dotted points show the observed excitations TP₁(k) at about $1.7 \times 10^7 \text{ m}^{-1}$ and TP₁($3k$) at $5.1 \times 10^7 \text{ m}^{-1}$.

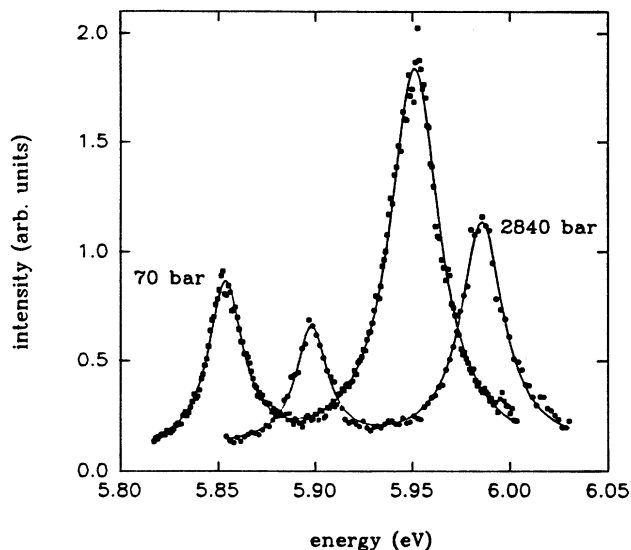


FIG. 2. Excitation spectra of RbI at 10 K for 70 and 2840 bars. The solid lines represent the nonlinear least-squares best fit.

($k=2\pi n/\lambda$) of the excitation is not known because of the strong dispersion of the complex index of refraction n near the absorption line and it is therefore difficult or even impossible to account for effects that depend on the size of the k vector, such as the mixing of heavy and light excitons.⁵ Therefore, they are often ignored. However, this problem is avoided by the use of multiphoton excitation where the k vectors used are small and essentially constant over the relevant range of excitation energies because each photon individually is far from any resonance, and hence interacts only weakly with the crystal. In this way excitations are observed with well-defined k vectors. The experimental setup has been previously described in more detail.² The freshly cleaved crystals were mounted in sapphire ball cells⁶ which were connected to a two-stage pressure generator and mounted to the coldhead of a closed-cycle refrigerator. Helium was used as the pressure medium because it ensured hydrostatic conditions for the sample.

Three-photon-excitation spectra were taken at pressures of 10, 2450, and 6010 bar with temperatures at 10, 25, 50, 75, and 100 K for KI and pressures of 70, 950, and 1990 bar with smaller temperature increments up to 100 K for RbI. The uncertainty in the pressure measurements is estimated to be about ± 10 bar. Successful population of the polariton states in question was observed by monitoring the luminescence emanating from the self-

trapped exciton. The intensity of the incoming light on the sample is estimated to be about 500 MW/cm^2 . The method of extracting the longitudinal and transverse excitonic energies from the data is described in detail in Refs. 2 and 3. The data for KI were fitted with the sum of two symmetric Lorentzians since none of the measurements, even at high temperature, revealed asymmetry. In RbI, the excitations began to show asymmetric behavior at temperatures higher than 70 K. Data for RbI at temperatures higher than 70 K were therefore excluded from the analysis. The asymmetry might be correlated with the Debye temperature of the crystals: 131 K for KI and 103 K for RbI.⁷ A temperature of 100 K for KI would still be substantially below the Debye temperature, whereas for RbI this would not be so.

III. RESULTS AND DISCUSSION

Figures 3(a) and 3(b) show the longitudinal exciton energies E_{1L} obtained from the Lorentzian best fits of data as shown in Fig. 2 for different temperatures at the three pressures. According to theory⁸ the self-energy of excitons weakly interacting with phonons is given by

$$\Sigma = \Delta_0 - i\Gamma_0, \quad (1)$$

and can be calculated in lowest approximation by the autocorrelation function of the interaction Hamiltonian H' between excitons and phonons. It turns out that both the real part Δ_0 and the imaginary part Γ_0 are proportional to a quantity D^2 which is defined as

$$D^2 = \sum_K |V_{K0}|^2 [2N(\hbar\omega_K) + 1], \quad (2)$$

and contains all the temperature dependence. $N(\hbar\omega_K)$ represents the usual Bose-Einstein phonon occupation number of $1/[\exp(\hbar\omega_K/kT) - 1]$ and V_{K0} denotes the interaction potential for the exciton-phonon coupling which is via their deformation potential for longitudinal-acoustic phonons and through Fröhlich coupling for longitudinal-optical phonons.

The resulting line shape of the excitation for the case of weak exciton-phonon coupling is found to be Lorentzian:

$$I(E) = \frac{A}{(E - \epsilon_0 - \Delta_0)^2 + \Gamma_0^2}, \quad (3)$$

where $I(E)$ denotes the intensity of the excitation depending on the energy E and ϵ_0 , the energy of the excitation without taking the exciton-phonon interaction into account. For low-lying Wannier exciton states, the real part of the self-energy Δ_0 has a negative value.⁹

In order to evaluate the above expressions one can try to approximate the actual phonon density of oscillators

TABLE I. 1s transverse and longitudinal energies and their pressure shifts at 10 K.

Crystal	E_{1L} (eV)	E_{1T} (eV)	$(\partial E_{1L}/\partial P)_{T=10}$ (meV/K)	$(\partial E_{1T}/\partial P)_{T=10}$ (meV/K)
KI	5.945 ± 0.001	5.846 ± 0.001	15.5 ± 0.2	16.0 ± 0.2
RbI	5.846 ± 0.001	5.748 ± 0.001	15.8 ± 0.5	16.3 ± 0.5

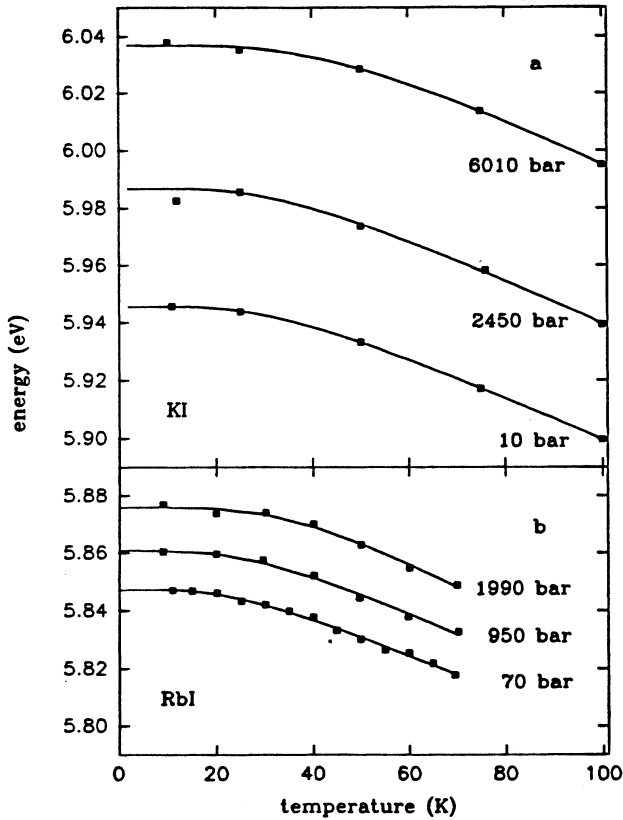


FIG. 3. (a) Energy of the first longitudinal exciton E_{1L} vs temperature for three different pressures. The datapoint at 10 K on the 2450 bars curve is actually not at 2450 bars, but at a slightly smaller pressure due to the pressure loss when the helium freezes (the system then moves along an isochore in the p - T plane). This had been anticipated for all other datapoints at temperatures for which the helium is frozen by increasing the pressure to a value higher than the one in the fluid phase to compensate for the pressure loss after freezing so that the pressure is the same as in the fluid phase. (b) the same as (a) for RbI.

by an ensemble of Einstein oscillators with an effective phonon energy $\hbar\Omega$. In this way the peak energy and its dependence on temperature can be written as

$$E_{\text{exciton}}(T) = (E_0 + \Delta) - \Delta \coth \left(\frac{\hbar\Omega}{2k_B T} \right), \quad (4)$$

where $\Delta = -\Delta_0(0)$ represents the energy shift arising from the exciton-phonon interaction at $T=0$ K and $E_0 = \varepsilon_0 + \Delta_0(0)$ stands for the excitonic energy at $T=0$ K. Equation (4) has been used in this form to express dependence of reflectivity maxima^{10,11} or of polariton peaks obtained by difference frequency generation.¹²

It has to be emphasized that the above theory deals with the behavior of excitons. What is actually measured are the energy and line shape of the exciton-polariton resonance and not that of the exciton itself. This does not affect the energy E_0 (which we also call E_{1T}) and the peak-shift parameter Δ , which are obtained by fitting Eq.

(4) [or later, Eq. (6)] to the data of Fig. 3 because E_{1T} is the energy of the 1s exciton. The linewidth parameter Γ poses more of a problem because it is not obvious that an exciton of wave vector k and the corresponding polariton (on the upper branch) with the same k have the same linewidth. Nevertheless the polaritons in KI and RbI on the upper branch are "excitonlike" (using a criterion of Hopfield¹³) for the k vector values that are relevant to our measurements (with energy E very close to E_{1L} and very small k values) meaning that they behave substantially like an exciton and not like a photon. Hopfield finds for these excitonlike polaritons that the scattering matrix elements between polariton states of wave vectors k and k' are the same as between excitonic states of the same wave vectors.¹³ Beyond the matrix elements however, it remains to be seen how the different density of states and the different group velocities which the polaritons have, affect the linewidth.¹³ Also, Beerwerth, Fröhlich, and Leinweber state that there are still problems in understanding the different linewidths for different excitons in alkali halides.¹⁴ Calculations within the charge-transfer exciton model¹⁵ indicate an intrinsic exciton linewidth parameter Γ of 0.44 meV for KI (0.53 meV for RbI) at a temperature of 5 K, which is much smaller than polariton linewidths measured by ourselves or reported by Beerwerth *et al.*¹⁶ The calculated values from Ref. 15 are actually much closer to the linewidth of polaritons on the lower branch with a k vector of about $12 \times 10^7 \text{ m}^{-1}$ as observed by Fröhlich *et al.* in Ref. 12. Therefore we conclude that the polariton linewidth measured by either one- or multiphoton techniques cannot be interpreted with certainty to be the intrinsic exciton linewidth.

The solid lines in Figs. 3(a) and 3(b) are the nonlinear least-squares best fit to the data. Tables II and III contain the values for E_{1L} and E_{1T} and the parameter values with their uncertainties (single standard deviation). Within experimental error there is no difference between the fitting parameters Δ , $\hbar\Omega$, and S for the longitudinal and transverse exciton [the quantity S indicates the strength of the exciton-phonon coupling (*vide infra*)].

An important aspect in the interpretation of the present dual pressure and temperature measurements is that the fit parameters E_0 , Δ , and $\hbar\Omega$ obtained by fitting, using Eq. (4), to the data contain both the effect of the lattice dilation with temperature and the change in self-energy with temperature at *constant volume*. It will be shown now that separating those contributions leads to significantly different results.

By elementary thermodynamic argument $(\partial E / \partial T)_v$ and $(\partial E / \partial T)_p$ are related as follows:

$$\left[\frac{\partial E}{\partial T} \right]_p = \left[\frac{\partial E}{\partial T} \right]_v - \beta_p(T) B_T(P) \left[\frac{\partial E}{\partial P} \right]_T, \quad (5)$$

with $\beta_p(T)$ the isobaric volume expansion coefficient and $B_T(P)$ the isothermal bulk modulus. This equation can be integrated and Eq. (4) can be substituted for the volume-dependent part of the energy. One thus obtains for the energy of the transverse 1s exciton,

TABLE II. Fit parameters of Eq. (4) for different pressures for the longitudinal exciton in KI in the top half; fit parameters of Eq. (4) for different pressures for the longitudinal exciton in RbI in the bottom half.

Pressure (bars)	$E_{1L}(0)$ (eV)	Δ_{1L} (meV)	$\hbar\Omega$ (meV)	S (meV/K)
10	5.946 ± 0.001	39 ± 2	8.6 ± 4	-0.79 ± 0.07
2450	5.987 ± 0.001	44 ± 12	9.2 ± 1.7	-0.84 ± 0.38
6010	6.037 ± 0.001	63 ± 13	12.0 ± 1.4	-0.90 ± 0.30
70	5.847 ± 0.001	26 ± 1	6.1 ± 0.7	-0.74 ± 0.15
950	5.861 ± 0.001	34 ± 11	7.3 ± 1.4	-0.80 ± 0.30
1990	5.876 ± 0.001	62 ± 24	10.2 ± 1.9	-1.04 ± 0.45

$$E_{1T}(T) = (E_0 + \Delta) - \Delta \coth \left[\frac{\hbar\Omega}{2k_B T} \right] - \int_0^T \left[\frac{\partial E_{1T}}{\partial P} \right]_T \beta_P(T') B_P(T') dT'. \quad (6)$$

Knowledge of the quantities under the integration sign would permit one to find the self-energy for constant volume. $\beta_P(T)$ has been measured at zero pressure for both KI and RbI.^{17,18} We assume that there are no significant changes over the pressure range of this study. The dependence of the bulk modulus B on pressure and temperature is also known by the behavior of the elastic constants.¹⁹ We found the pressure derivative $(\partial E_{1T}/\partial P)_T$ by grouping our results according to temperature. Since we have three values of $E_{1T}(p)$ for each of the temperatures, we can calculate $(\partial E/\partial P)_T$ for each temperature. Table IV lists the parameters of the pressure shift and the offset energy $E_{1T}(p=0)$ for the different temperatures. All uncertainties are single standard deviation. It turns out that $(\partial E/\partial P)_T$ is independent of temperature in the range up to 100 K for KI and 70 K for RbI within experimental uncertainty. One might be able to see a trend toward bigger pressure shifts with higher temperatures, especially for KI, but the differences are not significant within the threefold standard deviation and may simply reflect the larger compressibility at higher temperatures. The unweighted average of the pressure shift for all temperatures is 16.1 meV/kbar for KI and 16.5 meV/kbar for RbI. This can

be compared with the $(\partial E/\partial P)_T = 17.0$ meV/kbar for KI found at 120 K by Yamada *et al.*¹¹ There is also a value of 24.9 meV/K measured for KI at room temperature (293 K) though this was found observing the pressure shift of the tail of the absorption edge.²⁰ Since $(\partial E_{1T}/\partial P)_T$ was found to be independent of temperature in our range, we can pull it in front of the integration. The bulk modulus B also is constant in this temperature range. Even though the elastic constant c_{11} decreases with temperature, c_{12} increases and keeps B approximately constant. The values of B were estimated by us using the data given in Ref. 19. In the case of KI we estimated $B = 133, 148,$ and 170 kbar for pressure of 10, 2450, and 6010 bars. In the case of RbI we used $B = 122, 129,$ and 135 kbar corresponding to our pressures of 70, 950, and 1990 bars.

Repeating the fitting procedure one obtains the values of Table V. We feel that these values for E_0 , Δ , and $\hbar\Omega$ are the most trustworthy because thermal effects which contribute only through lattice dilation are accounted for separately.

A very similar approach has been used by Tomiki, Miyata, and Tsukamoto.¹⁰ Instead of Eq. (6) they used the following expression to correct for the contribution due to lattice dilation:

$$E_{1T}(T) = (E_0 + \Delta) - \Delta \coth \left[\frac{\hbar\Omega}{2k_B T} \right] - \frac{\alpha_M e^2}{a_0} \int_0^T \alpha(T') dT'. \quad (7)$$

TABLE III. Fit parameters of Eq. (4) for different pressures for the transverse exciton in KI in the top half; fit parameters of Eq. (4) for different pressures for the transverse exciton in RbI in the bottom half.

Pressure (bars)	$E_{1T}(0)$ (eV)	Δ_{1T} (meV)	$\hbar\Omega$ (meV)	S (meV/K)
10	5.847 ± 0.001	38 ± 3	8.6 ± 0.4	-0.77 ± 0.07
2450	5.889 ± 0.001	44 ± 13	9.2 ± 1.8	-0.82 ± 0.39
6010	5.941 ± 0.001	62 ± 14	12.0 ± 1.5	-0.89 ± 0.30
70	5.749 ± 0.001	26 ± 5	6.2 ± 0.7	-0.72 ± 0.22
950	5.763 ± 0.001	34 ± 11	7.3 ± 1.4	-0.80 ± 0.41
1990	5.779 ± 0.001	61 ± 24	10.3 ± 1.7	-1.02 ± 0.57

TABLE IV. Transverse exciton energy and its isothermal pressure shift for temperatures from 10 to 100 K for KI in the top half; transverse exciton energy and its isothermal pressure shift for temperatures from 10 to 70 K for RbI in the bottom half.

Temperature (K)	$E_{1T}(p=0)$ (eV)	$(\partial E/\partial P)_T$ (meV/kbar)
10	5.846±0.001	15.9±0.2
25	5.846±0.003	15.6±0.8
50	5.835±0.002	16.3±0.4
75	5.819±0.002	16.5±0.4
100	5.802±0.001	16.4±0.2
10	5.748±0.001	16.1±0.2
20	5.747±0.001	14.9±0.6
30	5.743±0.001	17.1±0.5
40	5.739±0.001	17.3±0.2
50	5.731±0.001	17.5±0.5
60	5.726±0.001	15.8±0.7
70	5.719±0.001	16.6±0.5

Only the last term is different with $\alpha(T')=\beta(T')/3$ representing the linear-expansion coefficient, α_M the Madelung constant of 1.747565 for NaCl structured crystals and a_0 the nearest-neighbor distance (3.51 Å in KI and 3.67 Å for RbI). It turns out that those two last terms are equivalent when one calculates the pressure dependence of the lowest-excitation energy using the model of Hilsch and Pohl.²¹ They have shown that this energy E_0 in alkali halide crystals can be rather well calculated by the empirical formula

$$E_0 = E_A - E_I + \frac{\alpha_M e^2}{a}, \quad (8)$$

with E_A the affinity of the halide (in our case iodine) and E_I the ionization energy of the alkali atom (in our case Rb and K). Assuming that E_A and E_I are independent of pressure, one can predict the pressure blueshift of E_0 by implementing the pressure dependence of $a \approx a_0(1-p/3B)$ with p as the pressure and B as the bulk modulus, obtaining $\alpha_M e^2/3Ba$ for the pressure shift. The pressure shift values obtained in this way are very close (within 13% in KI and 15% in RbI) to the experimentally observed ones.^{2,3} Substituting $\alpha_M e^2/3Ba$ for

$(\partial E_{1T}/\partial P)_T$ into Eq. (6), one can see the formal equivalence. When we fitted Eq. (7) to our data, we found values for the fit parameters that were almost the same as the ones obtained using Eq. (6) for the fitting.

For the following, we will discuss the fit parameters of Eq. (6) although the general conclusions are also valid for the fit parameters obtained with Eq. (4). One can observe these trends with pressure: (a) increase of $E_{1T}(0)$ and $E_{1L}(0)$ which was already stated for KI in a previous paper,² (b) increase of the effective phonon energy $\hbar\Omega$ with pressure, (c) increase of the absolute value of the real part of the self-energy Δ of the $n=1$ exciton. The calculated zero-pressure values for the real part of the self-energy Δ (14.7 meV for KI and 10.6 meV for RbI, Ref. 15) are slightly less than our measured low-pressure values of 25 meV (KI) and 16 meV (RbI) but the agreement is regarded as satisfactory considering the approximations involved (e.g., single-phonon frequency). (Reference 15 reports the values with a negative sign due to the different definition of the self-energy as already mentioned previously.)

One might try to interpret the results in terms of phonon-dispersion relations experimentally obtained by using inelastic-neutron scattering.^{22,23} The low-pressure values of 7.9 meV (KI) and 5.4 meV (RbI) for $\hbar\Omega$ seem to indicate that the phonons contributing to the excitonic self-energy are mainly LA phonons near the L -point singularity of the Brillouin zone of KI. Other candidates might be LA phonons with a k vector halfway to the K point or halfway to the X point. This appears to rule out the substantial participation of optical branches that are at energies higher than 12 meV (KI) or about 8 meV (RbI). Nevertheless other publications list effective phonon energies from 4.81 to 12.9 meV for KI (see Table VI) at zero pressure, which will lead one to different conclusions.¹⁰ However, the values reported in Ref. 10 were obtained by analyzing optical conductivity spectra using one-photon reflection spectroscopy. This technique is very sensitive to surface properties and the peak positions obtained by reflection spectroscopy are not at the resonant energies themselves. In addition, the values reported in Ref. 12 were obtained by nonlinear difference frequency generation spectra on the lower polariton branch using an iterative approach to evaluate the data that neglected temperature dependences of higher electronic energies.

TABLE V. Fit parameters of Eq. (6) for different pressures for the transverse exciton in KI in the top half; fit parameters of Eq. (6) for different pressures for the transverse exciton in RbI in the bottom half.

Pressure (bars)	$E_{1T}(0)$ (eV)	Δ_{1T} (meV)	$\hbar\Omega$ (meV)	S (meV/K)
10	5.847±0.001	25±2	7.9±0.4	-0.55±0.006
2450	5.889±0.001	27±4	8.3±0.7	-0.56±0.11
6010	5.941±0.001	46±14	13.0±2.1	-0.61±0.29
70	5.749±0.001	16±4	5.4±0.9	-0.51±0.20
950	5.763±0.001	25±10	7.2±1.7	-0.60±0.38
1990	5.779±0.001	50±26	10.6 ±2.6	-0.81±0.62

TABLE VI. Comparison of low-pressure values for $E(0)$, Δ , $\hbar\Omega$, and S obtained by fitting with Eq. (6) with values of other references.

Reference	$E(0)$ (eV)	Δ (meV)	$\hbar\Omega$ (meV)	S (meV/K)
10	5.8646	18.3	4.81	-0.98
12	5.847	74.1	12.9	-0.986
Our	5.847	25	7.9	-0.55

Another datum shown in the tables is the quantity $S = [\partial E(T)/\partial T]_{T \rightarrow \infty}$, which is the slope in the limit of high temperature. If the volume is kept constant [in our case this is achieved by fitting with Eq. (6)] S can also be written as

$$S = -\frac{2k_B \Delta}{\hbar\Omega} = \left[\frac{\partial E(T)}{\partial T} \right]_V, \quad T > 100 \text{ K}. \quad (9)$$

S characterizes the strength of the electron-phonon coupling.¹⁰ Our measurements therefore indicate that the absolute value of the coupling strength increases with pressure. The parameters obtained using Eq. (4) will give a limiting slope at constant pressure (-0.77 meV/K for KI and -0.72 meV/K for RbI in our case). These values are larger in magnitude than those for constant volume. They may be compared with other measurements for S at constant pressure. For KI, Refs. 10 and 12 find -0.98 meV/K. Haupt²⁴ obtains a value of -0.834 meV/K (absorption spectroscopy) and Guizzetti, Nosenzo, and Regguzoni²⁵ find -0.85 meV/K (thermoreflectivity method). For RbI, Ref. 25 states a value of -0.5 meV/K.

Our low-pressure values using the parameters of Table V, for S at constant volume (-0.55 meV/K for KI and -0.51 meV/K for RbI) are smaller than the -0.72 meV/K (KI) found in Ref. 10 or the -0.63 meV/K (KI) found in Ref. 11. In order to facilitate an overall comparison of the low-pressure values Table VI lists the values from Refs. 10 and 12 and our measurements.

A. $n = 1$ Half-width [TP(k) and TP($3k$)]

This section deals with the half-width of the two transverse polaritons TP₁(k) and TP₁($3k$) on the upper polariton branch that we observe. In general, the linewidths of the TP₁(k) and TP₁($3k$) decrease with pressure at low temperature (10 K) for both KI and RbI. The decrease in linewidth for both TP₁(k) and TP₁($3k$) for both substances is about the same, approximately -1.3 meV/kbar. The data are scattered, which is the reason that the linewidth for RbI in Table VII seems to increase although a thorough separate investigation using data-points at several different pressures shows that this is not the case. Figure 4 shows these half-width data of RbI for the TP₁(k) and the TP₁($3k$). Figures 5(a) and 5(b) show the FWHM linewidth of KI and RbI versus temperature for the three different pressures. It can be seen that the half-width stays constant to about 25 K and then increases rapidly to almost twice its low-temperature value at 100 K. Within the Einstein approximation for the fre-

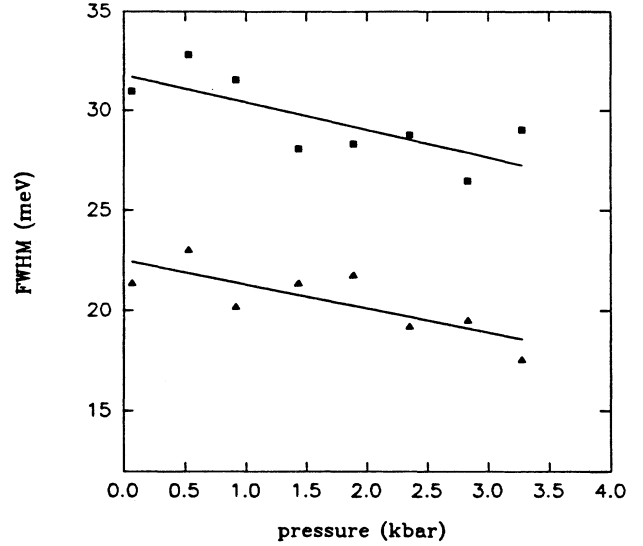


FIG. 4. Pressure dependence of the linewidth of the TP₁(k) (triangles) and the TP₁($3k$) (solid squares) in RbI at a temperature of 9 K.

quency spectrum of the phonons the half-width of the exciton depends on temperature with the same functional form used to describe the temperature dependence of the excitonic energy.⁸ We will use this form to describe the half-width of the exciton-polariton resonance as follows:

$$2\Gamma(T) = 2\Gamma(0) \coth \left[\frac{\hbar\Omega}{2k_B T} \right]. \quad (10)$$

Table VII lists the fit parameters together with their uncertainties (single standard deviation).

For KI we find the following. The effective phonon energy $\hbar\Omega_K$ of the phonons involved in the decay of the transverse polariton TP₁(k) basically stays constant whereas the effective phonon energy $\hbar\Omega_{3k}$ connected with the decay of the TP₁($3k$) decreases with increasing pressure. Also the (effective) phonons responsible for the decay of the excitation at higher temperatures are different from the ones contributing to the excitonic self-energy. According to the theory,⁸ the temperature behavior should be the same for self-energy and linewidth. The discrepancy might again be due to the fact that we are dealing with the linewidth of the polariton and not that of the exciton.

One can also try to interpret these results with the help of the phonon-dispersion relations and their density of states.^{22,23} The effective energy of the phonons involved with the decay of the TP₁(k) lies in the gap separating the acoustical and optical branches and therefore one might assume that longitudinal-optical (at the X and K points of the Brillouin zone) as well as longitudinal-acoustical phonons at the L zone boundary or halfway to the X or K points are contributing to the decay.

The phonons responsible for the decay of the TP₁($3k$) could be LO phonons at the X and K zone boundaries and/or again the same LA phonons as in the case of the

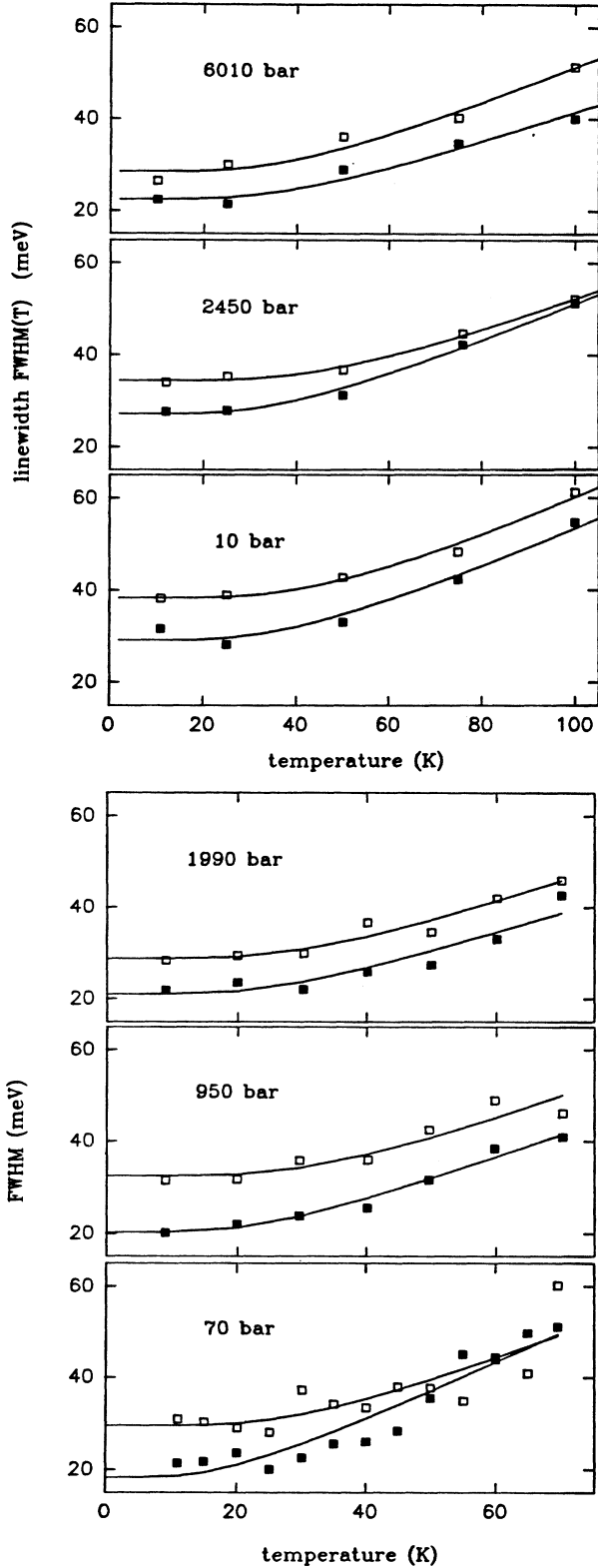


FIG. 5. (a) Linewidth (FWHM) of the $TP_1(k)$ (solid squares) and of the $TP_1(3k)$ (hollow squares) vs temperature at pressures of 10, 2450, and 6010 bars for KI and (b) the same for RbI at pressures of 70, 950, and 1990 bars. The solid lines represent the best fit of Eq. (10) to the data.

TABLE VII. Fit parameters of Eq. (9) for the $TP(k)$ and $TP(3k)$ at several pressures for KI in the top half; fit parameters of Eq. (9) for the $TP(k)$ and $TP(3k)$ at several pressures for RbI in the bottom half.

Pressure (bars)		$2\Gamma(0)$ (meV)	$\hbar\Omega$ (meV)
10	$TP(k)$	29.1 ± 1.5	10.5 ± 0.9
	$TP(3k)$	38.4 ± 0.9	13.0 ± 0.6
2450	$TP(k)$	27.2 ± 0.8	10.2 ± 0.5
	$TP(3k)$	34.4 ± 0.5	13.6 ± 0.4
6010	$TP(k)$	22.5 ± 1.3	10.5 ± 0.9
	$TP(3k)$	28.6 ± 1.5	10.8 ± 1.0
70	$TP(k)$	18.4 ± 2.3	4.7 ± 0.8
	$TP(3k)$	29.6 ± 2.3	8.4 ± 1.3
950	$TP(k)$	20.3 ± 1.0	6.5 ± 0.5
	$TP(3k)$	32.5 ± 1.7	9.4 ± 1.1
1990	$TP(k)$	21.0 ± 1.8	7.3 ± 1.0
	$TP(3k)$	28.8 ± 1.2	8.9 ± 0.8

$TP_1(k)$ together with LO phonons at the Γ point.

For RbI we find that the effective phonon energy increases with pressure for the $TP_1(k)$, whereas for the $TP_1(3k)$ it remains approximately constant. The phonons contributing to the self-energy of RbI at higher temperature have the same energy as those responsible for the decay of the $TP_1(k)$ at higher temperature within the uncertainty and show the same increase in pressure. The participating phonons might be more of an acoustic nature for the $TP_1(k)$ or could also be LO phonons at the zone boundaries, but not the larger energy phonons at the Γ point.

IV. CONCLUSION

In conclusion we have measured the $1s$ exciton energies in KI and RbI versus temperature up to 100 K for three different pressures (10, 2450, and 6010 bar for KI and 70, 950, and 1990 bar for RbI). Excitons and phonons in KI and RbI couple only weakly, which results in the Lorentzian line shape of the polaritons. At temperatures close to the Debye temperature, the Lorentzian line shapes became asymmetric. It would be interesting to look in detail at even higher temperatures to seek the cause of the asymmetry. Within the framework of the weak-coupling model we found the dependence of the peak-shift parameter Δ (real part of the self-energy of the exciton) on pressure and the behavior of the linewidth with temperature and pressure. Our results indicate that the absolute value of the real part of the self-energy rises with pressure and that the effective phonon energies contributing to the peak shift also grow with pressure. Excitons couple more strongly to the phonons with pressure as described by an increase of the absolute value of the parameter $S = (\partial E / \partial T)_v$. The change of the effective energy of the phonons contributing to the exciton self-energy would correspond to Grüneisen parameters γ of

about 10 for KI and even about 50 for RbI. Within the reliability of such a simple model of the phonon spectrum, the nonordinary values of *shift* of effective phonon energy with pressure suggest that the “dominant phonons” participating in the process change *within* the phonon spectrum as pressure is changed. It may be worth noting that an assumption that all acoustic-phonon modes couple equivalently, which would suggest use of a

Debye spectrum, may be ruled out because the functional form would significantly deviate from the observed temperature dependences.

ACKNOWLEDGMENT

This work was partially supported by the National Science Foundation through Grant No. DMR-8822639.

*Present address: Institut für Physik der Universität Dortmund, 4600 Dortmund, Germany.

¹F. Beerwerth and D. Fröhlich, *Phys. Rev. Lett.* **55**, 2603 (1985).

²M. J. Lipp and W. B. Daniels, *Phys. Rev. Lett.* **67**, 2810 (1991).

³J. Blechschmidt, M.S. thesis, University of Delaware, 1992.

⁴M. J. Lipp and W. B. Daniels, *Phys. Rev. B* **47**, 6931 (1993).

⁵G. Fishman, *Solid State Commun.* **27**, 1097 (1978).

⁶W. B. Daniels, M. Lipp, D. Strachan, D. Winters, and Z. Yu, in *Recent Trends in High Pressure Research*, Proceedings of the XIII AIRAPT International Conference on High Pressure Science and Technology, edited by A. K. Singh (Oxford and IBH, New Delhi, 1992), p. 809.

⁷J. T. Lewis, A. Lehoczky, and C. V. Briscoe, *Phys. Rev.* **161**, 877 (1967).

⁸S. Nakajima, Y. Toyozawa, and R. Abe, *The Physics of Elementary Excitations*, Springer Series in Solid State Sciences Vol. 12 (Springer-Verlag, Berlin, 1980).

⁹R. S. Knox, in *Theory of Excitons*, edited by F. Seitz and D. Turnbull (Academic, New York, 1963), p. 154.

¹⁰T. Tomiki, T. Miyata, and H. Tsukamoto, *Z. Naturforsch* **29**, 145 (1974).

¹¹A. Yamada, H. Fukutani, M. Miyabe, K. Yagi, H. Kato, T. Koide, T. Shidara, T. Miyahara, and S. Sato, *J. Phys. Soc. Jpn.* **54**, 4005 (1985).

¹²D. Fröhlich, P. Köhler, W. Nieswand, T. Rappen, and E.

Mohler, *Phys. Rev. B* **43**, 12 590 (1991).

¹³J. J. Hopfield, *Phys. Rev.* **182**, 945 (1969).

¹⁴F. Beerwerth, D. Fröhlich, and V. Leinweber, *Phys. Status Solidi B* **145**, 195 (1988).

¹⁵H. Zheng and J. Fang, *Acta. Phys. Sin. Abst.* **36**, 339 (1987) [*Chin. J. Phys.* **8**, 32 (1988)].

¹⁶F. Beerwerth, D. Fröhlich, P. Köhler, V. Leinweber, and A. Voss, *Phys. Rev. B* **38**, 4250 (1988).

¹⁷B. Yates and C. H. Panter, *Proc. Phys. Soc. London* **80**, 373 (1962).

¹⁸G. K. White and J. G. Collins, *Proc. Soc. London Ser. A* **333**, 237 (1973).

¹⁹*Numerical Data and Functional Relationships in Science and Technology*, Landolt-Börnstein, New Series, Group III, Vol. 11 (Springer, Berlin, 1979), Chap. 1.

²⁰T. Masuzaki, T. Shika, and S. Masunaga, *J. Phys. Soc. Jpn.* **59**, 3021 (1990).

²¹R. Hilsch and R. W. Pohl, *Z. Phys.* **57**, 145 (1929).

²²G. Dolling, R. A. Cowley, C. Schittenhelm, and J. M. Thorson, *Phys. Rev.* **145**, 577 (1966).

²³G. Raunio and S. Rolandson, *Phys. Status Solidi* **40**, 749 (1970).

²⁴U. Haupt, *Z. Phys.* **157**, 232 (1959).

²⁵G. Guizzetti, L. Nosenzo, and E. Reguzzoni, *Phys. Rev. B* **15**, 5921 (1977).